Agrotechniques in Industrial Crops

Journal Homepage: https://atic.razi.ac.ir

# Development of WPI/Gelatin Active Films Loaded with *Cuminum cyminum* Essential Oil Nanoemulsion for the Control of *Sitophilus oryzae*

**Maryam Shahnazari, Alireza Jalalizand*, Esmaeil Mahmoudi**

*Department of Plant Protection, Faculty of Agriculture, Water, Food and Nutraceuticals, Isf.C., Islamic Azad University, Isfahan, Iran*

**ARTICLE INFO**

***Original paper***

*Article history:*
Received: xx xxx 202x
Revised: xx xxx 202x
Accepted: xx xxx 202x

*Keywords:*
Acetylcholinesterase inhibition
Active packaging
*Cuminum cyminum*
Glutathione S-transferase
*Sitophilus oryzae*

**ABSTRACT**

Protecting stored cereals against the rice weevil (*Sitophilus oryzae*) remains a key challenge in stored-product entomology. Biodegradable packaging has emerged as a sustainable strategy for postharvest pest management. This study developed active edible films from gelatin and whey protein isolate with *Cuminum cyminum* essential oil nanoemulsions at 0.1, 0.25, and 0.5% w/w via ultrasound. The films were fabricated via solution casting and thoroughly characterized by dynamic light scattering (DLS), scanning electron microscopy (SEM), Fourier-transform infrared spectroscopy (FTIR), as well as mechanical and barrier property tests. Insecticidal bioassays included fumigant toxicity, repellency, larval penetration tests, and enzymatic assays for glutathione S-transferase (GST) and acetylcholinesterase (AChE) activity. DLS analysis revealed that the nanoemulsion at 0.25% concentration exhibited a mean droplet size of 47.94 nm with a polydispersity index (PDI) of 0.230, indicating a stable and relatively monodisperse system. SEM micrographs confirmed the uniform distribution of nanoemulsion droplets within the film matrix. Increasing the nanoemulsion concentration significantly improved the tensile strength (TS) from 18.0 to 20.1 MPa and reduced the water vapor permeability (WVP) from 0.98 to 0.85 × $10^{-10}$ g.m$^{-1}$.s$^{-1}$ Pa$^{-1}$. The film containing 0.5% nanoemulsion exhibited the highest fumigant toxicity against larvae, with an $LC_{50}$ value of 0.559 µL L$^{-1}$ air. The repellency index (RI) for larvae reached 87% at the 0.25% concentration. Furthermore, the 0.25% cumin nanoemulsion resulted in the absence of normal GST activity in all tested insects and significantly reduced AChE activity, suggesting a dual disruptive effect on the insect's detoxification and neural systems. Collectively, these findings demonstrate that active edible films loaded with *C. cyminum* nanoemulsions exhibited favorable mechanical strength and moisture-barrier properties, together with repellency (up to 87%) and fumigant activity (up to 92.8% mortality), as well as enzyme-inhibitory effects against *S. oryzae*. Therefore, they offer a promising, sustainable, and eco-friendly alternative for integrated pest management (IPM) of stored-grain pests.

DOI: 10.22126/ATIC.2027.14251.1296
© The Author(s) 202x. Published by Razi University

## 1. Introduction

*Cuminum cyminum* L. (cumin), a member of the Apiaceae family, is one of the oldest and most economically important medicinal plants cultivated worldwide (Moradi and Piri, 2018). It is extensively grown in arid and semi-arid regions, particularly in Iran, India, China, Egypt, Turkey, and Mediterranean countries, where it is widely used as a culinary spice and medicinal plant. Cumin has long been used in traditional medicine because of its diverse biological activities, including antioxidant, antimicrobial, and anti-inflammatory properties, which are largely attributed to its biologically active essential oil constituents. The essential oil of cumin is particularly rich in monoterpenes and oxygenated terpenoids, with cuminaldehyde being the dominant bioactive compound accompanied by γ-terpinene, *p*-cymene, β-pinene, and other volatile constituents. These phytochemicals exhibit a broad spectrum of biological activities, including antimicrobial, antifungal, insecticidal, and repellent effects, making cumin essential oil an attractive natural alternative to synthetic pesticides (Demeter *et al*., 2021; Jalaeian *et al*., 2021). Owing to its high biological activity, low mammalian toxicity, and biodegradability, cumin essential oil has recently attracted considerable attention for

* Corresponding author.
E-mail address: a.jalalizand@iau.ac.ir

applications in sustainable agriculture, food preservation, and eco-friendly pest management (Ashraf *et al*., 2021; Sandberg *et al*., 2023).

Despite its remarkable biological potential, the practical application of cumin essential oil remains limited because of its instability, including high volatility, susceptibility to oxidation and photodegradation, and poor environmental stability. These limitations considerably reduce its persistence and insecticidal efficacy during storage and commercial application. Consequently, formulation technology has become a critical factor in improving the stability, controlled release, and biological performance of plant-derived essential oils (He *et al*., 2024). Among various botanical insecticides, comparative evaluations of twenty-five essential oils demonstrated that cumin essential oil exhibited one of the strongest repellent activities against the rice weevil, *Sitophilus oryzae*, while also representing a cost-effective botanical resource suitable for practical application (Demeter *et al*., 2021; Jalaeian *et al*., 2021). Therefore, developing advanced delivery systems capable of protecting cumin essential oil against rapid degradation while maintaining its biological activity represents an important research priority.

Rice (*Oryza sativa* L.) is one of the world's most important cereal crops and serves as the staple food for more than half of the global population, particularly in developing countries (Zhou *et al*., 2021). However, substantial postharvest losses occur during storage due to insect infestations, making the protection of stored rice a major challenge for food security and grain quality. Therefore, developing effective and environmentally friendly strategies for stored-grain pest management is of considerable importance.

Among the most destructive insects attacking stored rice is the rice weevil, *S. oryzae* (Coleoptera: Curculionidae), which causes severe quantitative and qualitative losses during post-harvest storage. Besides direct grain consumption, infestations facilitate secondary contamination by fungi and bacteria, thereby reducing both grain quality and market value (Chaudhari *et al*., 2021). Adults measure approximately 3–5 mm in length and possess characteristic circular punctures on the pronotum. Unlike the granary weevil, *S. oryzae* is widely distributed throughout tropical and subtropical regions, including India, Australia, the Mediterranean Basin, the Middle East, and the Americas. Although adults continue feeding throughout their lifespan, the larval stage is responsible for the greatest economic damage because larvae complete their development inside cereal kernels. Adult longevity ranges from four to five months and may occasionally extend to eight months, during which a single female can oviposit between 400 and 576 eggs (Baqeri Zanouz, 1999).

Post-harvest losses caused by stored-product insects continue to represent a major challenge worldwide (Meybeck *et al*., 2011). Since the 1960s, chemical insecticides have served as the principal strategy for controlling storage pests (Doherty *et al*., 2023). However, excessive dependence on synthetic pesticides has resulted in several environmental and public health concerns, including insecticide resistance, toxic residue accumulation in food and the environment, and risks to human health and ecological safety (Attia *et al*., 2020). Consequently, considerable research efforts have focused on identifying environmentally friendly alternatives capable of replacing or reducing conventional pesticides (Demeter *et al*., 2021). Plant-derived essential oils have emerged as promising botanical pesticides because of their rapid biodegradation, low toxicity toward mammals, and diverse biological activities (Ashraf *et al*., 2021). Their major constituents, particularly terpenoids, exhibit strong fumigant, contact toxic, and repellent activities against numerous insect pests (Sandberg *et al*., 2023).

Nevertheless, the commercial application of essential oils remains constrained by their inherent physicochemical instability. Nanoformulation technologies, especially nanoemulsions, have recently received considerable attention because they enhance the stability, dispersion, controlled release, and persistence of volatile bioactive compounds while improving insecticidal performance (He *et al*., 2024). Incorporating essential oil nanoemulsions into biodegradable active packaging materials protects volatile compounds from degradation. It also enables the prolonged release of insecticidal constituents during storage (Kavallieratos *et al*., 2023; Johnson *et al*., 2022). Active packaging systems, in which natural bioactive compounds are integrated into biodegradable polymer matrices, represent an environmentally sustainable alternative to petroleum-based plastics whose persistence has become a major environmental concern (Daliri Shamsabadi, 2023). Such packaging

not only extends food shelf life but also preserves quality by providing continuous antimicrobial and insect-repellent protection (Açıkgöz, 2020; Marsin *et al*., 2020; Aghajani *et al*., 2024). Furthermore, stable nanoemulsions incorporated into edible films can improve barrier properties through effective integration of hydrocolloid and lipid phases (Adak *et al*., 2020).

Blending biodegradable biopolymers is an effective strategy for enhancing the mechanical and barrier properties of edible films. Gelatin readily forms cross-linked networks with proteins, whereas whey protein isolate (WPI) provides excellent elasticity and film-forming capacity, making the WPI/gelatin combination particularly suitable for developing biodegradable active packaging materials (Aider, 2010). Previous studies have demonstrated that edible films containing plant essential oils can effectively repel stored-product insects (Marsin *et al*., 2020). For example, bilayer chitosan/WPI films incorporating cumin essential oil exhibited improved morphological characteristics and good potential for practical applications (Hosseinzadeh *et al*., 2021). Likewise, polylactic acid (PLA)-based edible films containing basil essential oil significantly reduced infestations of *S. oryzae* (Prabhakar *et al*., 2024).

In addition to their fumigant and repellent properties, plant essential oils exert insecticidal activity by interfering with essential biochemical pathways. Numerous terpenoid constituents inhibit key detoxification and neurotransmission enzymes, particularly acetylcholinesterase (AChE) and glutathione S-transferase (GST) (Piri *et al*., 2021). GSTs constitute a multifunctional enzyme family involved in xenobiotic detoxification, intracellular transport, and protection against oxidative stress. Because GST-mediated detoxification represents one of the principal defense mechanisms of insects against insecticides, inhibition of this enzyme considerably enhances the susceptibility of insects to botanical pesticides (Dastranj *et al*., 2017). Accordingly, investigating the effects of cumin essential oil on GST activity provides valuable insight into its insecticidal mode of action.

Whey protein isolate (WPI) and gelatin were selected because they possess complementary physicochemical characteristics that are advantageous for the fabrication of active biodegradable films. WPI provides excellent film-forming ability, favorable mechanical strength, and good oxygen barrier properties, whereas gelatin contributes flexibility, biocompatibility, and compatibility with bioactive compounds such as essential oils. The combination of these biopolymers results in a balanced film matrix with improved functional performance for active food-packaging applications. Furthermore, both materials are biodegradable, readily available, and economically attractive, making them suitable candidates for the development of sustainable packaging systems.

Therefore, the present study aimed to develop biodegradable WPI/gelatin active films incorporating nanoemulsified *C. cyminum* essential oil and to thoroughly evaluate their physicochemical characteristics and insecticidal efficacy against *S. oryzae*. Particular emphasis was placed on their repellency, fumigant toxicity, larval penetration inhibition, and biochemical mode of action through the inhibition of glutathione S-transferase (GST) and acetylcholinesterase (AChE), thereby providing a sustainable botanical packaging strategy for the protection of stored rice.

## 2. Materials and methods

### *2.1. Chemicals and essential oil extraction*

Whey protein isolate (WPI), gelatin, glycerol, and Tween 80 were supplied by Merck (Darmstadt, Germany). The dried fruits of *C. cyminum*. were purchased from a local herbal market in Isfahan, Iran, and were commercially labeled as originating from Kerman Province, Iran. Since the plant material was obtained in its commercially dried form, the drying conditions (temperature and duration) were not available. The dried fruits were ground into powder, and the essential oil was extracted by hydrodistillation using a Clevenger-type apparatus for 3 h. The extracted oil was dehydrated over anhydrous sodium sulfate, filtered, and stored in amber glass vials at 4 °C until further analysis.

### *2.2. GC–MS analysis of essential oil composition*

Chemical profiling of the cumin essential oil was performed using a gas chromatograph (Agilent, USA) coupled to a mass spectrometer (MS), equipped with an Rtx-5ms capillary column (30 m × 0.25 mm i.d., 0.25 μm film thickness). Helium was used as the carrier gas at a constant flow rate of 1.0 mL $min^{-1}$. The oven temperature program was initiated at 60°C (held for

4 min), increased to 290°C at a rate of 10°C $min^{-1}$, and maintained at 290 °C for 3 min. The injector and detector temperatures were set at 250 °C and 280 °C, respectively. One microliter (1 µL) of the essential oil sample was injected into the GC–MS system using a split ratio of 1:20. Mass spectra were recorded in electron impact (EI) mode at 70 eV over a mass range of 40–450 m/z. Compound identification was accomplished by comparing mass spectral data with those of authentic standards, as well as by matching calculated retention indices with values reported in the literature (Adams, 2007) and the NIST mass spectral library. Relative percentage compositions were determined using the peak area normalization method (Msegued Ayam *et al*., 2025).

### *2.3. Insect rearing*

A primary colony of *S. oryzae* was obtained from a stored-grain warehouse and authenticated by the Iranian Research Institute of Plant Protection. Rearing was conducted following standard laboratory procedures described by Strong et al. (1967). Confiroz rice grains were pre-treated at –20°C for 72 h to eliminate any hidden infestation. Insects were maintained in 200-mL plastic containers at 27 ± 1°C and 65 ± 5% relative humidity (RH) under complete darkness. To obtain synchronized populations, adults were allowed to oviposit for 3–5 days, after which the grains were sieved. First-generation adults (1–7 days old) and first-instar larvae were used for all bioassays (Bhanderi, 2012).

### *2.4. Preparation of nanoemulsions and active films*

To encapsulate the essential oil and enhance its stability, a high-energy ultrasonication method was employed (Peng *et al*., 2024). Oil-in-water nanoemulsions were prepared by mixing cumin essential oil with 0.1% Tween 80 solution at an essential oil-to-emulsifier ratio of 1:1 (v/v). The nanoemulsions were prepared at three essential oil concentrations of 0.1, 0.25, and 0.5% (w/w). Ultrasonication was performed using a titanium probe (MTI, Switzerland; 400 W, 20.5 kHz) at 30% amplitude for 15 min.

Active edible films were fabricated via the solvent casting method using a polymer matrix composed of WPI and gelatin at a 1:1 (w/w) ratio, selected for their cohesive network and biodegradability (Yarahmadi *et al*., 2024). Glycerol was added as a plasticizer at a fixed ratio. The ternary interactions among biopolymers were optimized based on Wang et al. (2026). The resulting mixture was degassed under vacuum for 24 h to remove entrapped air bubbles, cast into standard molds, and dried at 25°C until complete solvent evaporation (Oliyaei *et al*., 2026).

### *2.5. Characterization of nanoemulsions and films*

#### *2.5.1. Dynamic light scattering (DLS)*

The mean droplet size and polydispersity index (PDI) of the nanoemulsions were determined at 25°C using a Bettersize Nanoparticle Analyzer (Bettersize Instruments Ltd.) based on the dynamic light scattering (DLS) technique. Prior to analysis, the nanoemulsion samples were diluted with distilled water, equilibrated for 120 s, and measured in glass cuvettes at a scattering angle of 90° and a wavelength of 671 nm (Peng *et al*., 2024).

#### *2.5.2. Scanning electron microscopy (SEM)*

Surface morphology and cross-sectional microstructure of the films were examined using scanning electron microscopy (SEM). Film samples were cryo-fractured in liquid nitrogen, sputter-coated with gold, and imaged at an appropriate accelerating voltage to confirm uniform nanoemulsion distribution within the polymer matrix. Quantitative SEM image analysis: In addition to qualitative observation, SEM micrographs were quantitatively analyzed using ImageJ software (National Institutes of Health, Bethesda, MD, USA). The scale of each image was calibrated according to the embedded scale bar. Clearly distinguishable dispersed domains were identified and measured using the Analyze Particles function. The equivalent circular diameter (ECD) of each domain was calculated from its projected area and expressed as mean ± standard deviation. Because the number of distinguishable domains in the available SEM micrographs was limited, the obtained values are presented only as complementary morphological information rather than a statistically representative particle-size distribution (Peng *et al*., 2024).

#### *2.5.3. Fourier-transform infrared spectroscopy (FTIR)*

Chemical functional groups and molecular interactions within the films were analyzed using a Fourier-transform infrared (FTIR) spectrometer

(PerkinElmer, USA, Spectrum Version 10.00.00). Spectra were recorded in the wavenumber range of 4000–450 $cm^{-1}$. Film samples were placed directly in the infrared beam path, and characteristic absorption bands were recorded to evaluate the effects of nanoemulsion incorporation into the WPI/gelatin matrix.

Quantitative analysis of the FTIR spectra was performed by comparing the characteristic absorption bands of the control and cumin essential oil-containing samples. Peak positions were determined directly from the spectra, and the corresponding shifts in wavenumber were calculated to evaluate possible molecular interactions between the WPI/gelatin matrix and the encapsulated essential oil constituents. The observed spectral changes were interpreted according to previously reported assignments of hydrogen bonding and functional-group interactions.

### *2.6. Physical and mechanical properties*

#### *2.6.1. Mechanical properties*

Tensile strength (TS) and elongation at break (EAB) were measured according to ASTM D882 using a universal testing machine (Instron, USA) at a crosshead speed of 10 mm $min^{-1}$. Film specimens (2 × 1 cm) with a thickness of 1 mm were conditioned under standard laboratory conditions prior to testing. The initial grip separation was adjusted according to ASTM D882. Four replicate specimens were tested for each formulation, and the average values of TS and EAB were reported (Wang *et al*., 2026).

#### *2.6.2. Water vapor permeability (WVP)*

WVP was determined gravimetrically following the ASTM E96 method at 25°C and 75% RH. Weight changes over time were recorded and used to calculate WVP according to Ji et al. (2026).

#### *2.6.3. Moisture content and solubility*

Moisture content was determined by drying pre-weighed film samples in a hot-air oven at 105 °C until constant weight was achieved. Moisture content was calculated as the percentage difference between the initial and final dry weights. Water solubility was determined by immersing pre-dried film samples in distilled water for 6 h at room temperature under gentle agitation. The undissolved residues were recovered, dried to constant weight, and weighed. Solubility was calculated as the percentage of dry matter lost during immersion according to the method described by Yarahmadi et al. (2024). All measurements were performed in triplicate, and the mean values were used for statistical analysis (Yarahmadi *et al*., 2024).

### *2.7. Insecticidal bioassays*

#### *2.7.1. Repellency index (RI)*

The repellency assay was conducted following the method of Jesser et al. (2022). A glass tube (20 cm length × 2 cm diameter) was divided into three equal zones: A (treated), B (neutral), and C (control). Film strips containing 0.1, 0.25, or 0.5% nanoemulsion were placed in zone A, while control films without nanoemulsion were placed in zone C. Sixty adult weevils or larvae were released into the central zone (B) of each tube. The tubes were maintained at 27 ± 1 °C, 65 ± 5% relative humidity, and continuous darkness throughout the 72 h experimental period. After 72 h, the number of insects present in each zone was recorded. Four independent replicates were performed for each treatment. The repellency index (RI) was calculated using Equation 1.

$$RI = (C - A) / (C + A) \quad (1)$$

Where C and A represent the number of insects in the control and treated zones, respectively. An RI>0.1 indicates repellent activity (Jesser *et al*., 2022).

#### *2.7.2. Fumigant toxicity*

Fumigant toxicity was evaluated using a modified method of Jasman et al. (2025). Film strips (1 × 2 cm) were attached to the inner surface of the lids of 50-mL glass vials. A thin mesh barrier was placed between the film and the insects to prevent direct contact while permitting exposure to volatile compounds released from the film. Each vial contained 60 adult weevils or larvae. The tested doses were defined according to the nominal concentration of nanoemulsion incorporated into the film-forming formulation (0.1, 0.25, and 0.5%, w/w), rather than the concentration of essential oil measured in the vial headspace. Control vials contained an equivalent WPI/gelatin film prepared without essential-oil nanoemulsion. Mortality was recorded at 3, 6, 9, 12, 24, 36, and 48 h after exposure. Insects that showed no response to gentle mechanical stimulation were considered dead (Omar *et al*., 2024). Each

concentration and the control were evaluated in four independent replicates. When control mortality occurred, mortality values were corrected using Abbott's formula (Equation 2). Median and 90% lethal concentrations ($LC_{50}$ and $LC_{90}$), expressed as the percentage of nanoemulsion incorporated into the film-forming formulation, and median and 90% lethal times ($LT_{50}$ and $LT_{90}$) were estimated by Probit analysis (Miller and Tainter, 1944).

(2) $$\text{Corrected mortality (\%)} = [(M_t - M_c)/(100 - M_c)] \times 100$$

$M_t$ is the observed mortality percentage in the treatment and $M_c$ is the observed mortality percentage in the control.

*2.7.3. Larval penetration test*

The ability of larvae to penetrate the films was assessed by placing a film disc between two compartments, with a food attractant in the lower compartment. Sixty larvae were released into the upper compartment of each test unit, and larval penetration through the film was monitored over 21 days. The number of larvae that penetrated the film was recorded, and the penetration rate was expressed as a percentage. Four independent replicates were performed for each treatment according to the method described by Jesser et al. (2022).

*2.8. Biochemical enzyme assays*

*2.8.1. Enzyme extraction*

Adult weevils and larvae were collected 24 h after treatment. For enzyme extraction, the insects were homogenized in cold distilled water at a ratio of four insects per millilitre. The homogenates were centrifuged at 13,000 rpm for 20 min at 4°C, and the resulting supernatants were stored at −20°C until enzyme activity assays. Cold distilled water was used during the extraction step according to the method described by Omar et al. (2024), whereas phosphate buffer was subsequently used in the reaction mixtures of the individual enzyme assays. A total of 4 independent biological replicates were prepared for each treatment and the control.

*2.8.2. Glutathione S-transferase (GST) assay*

GST activity was measured spectrophotometrically using 1-chloro-2,4-dinitrobenzene (CDNB) as the substrate (Habig *et al*., 1974). The reaction mixture contained phosphate buffer, reduced glutathione (GSH), and CDNB. The enzyme extract was added, and the mixture was incubated for 5 min at 25°C. Absorbance was recorded at 340 nm using a UV–Vis spectrophotometer.

*2.8.3. Acetylcholinesterase (AChE) assay*

AChE activity was determined using a standard colorimetric method based on Ellman's assay (Ellman *et al*., 1961). The reaction mixture contained phosphate buffer, acetylthiocholine iodide (substrate), and 5,5′-dithiobis(2-nitrobenzoic acid) (DTNB). Enzyme extract was added, and the change in absorbance was monitored at 412 nm over 5 min. Enzyme activities were expressed as units per mg of protein.

*2.9. Statistical analysis*

Toxicity indices (LC and LT values) with 95% confidence limits were determined by Probit analysis. Model fit was assessed using the chi-square ($\chi^2$) test. For physicochemical and enzymatic data, one-way analysis of variance (ANOVA) was performed, followed by Duncan's multiple range test (DMRT) for mean comparisons. All statistical analyses were conducted using SPSS version 26.0 (IBM, USA) and Microsoft Excel 2024. Differences were considered significant at $p<0.05$ (Jasman *et al*., 2025).

## 3. Results and discussion

According to the GC–MS analysis, the essential oil of *C. cyminum* was predominantly composed of γ-terpinen-7-al (30.51%), also known as p-mentha-1,4-dien-7-al (IUPAC: 4-propan-2-ylcyclohexa-1,4-diene-1-carbaldehyde; CAS No. 22580-90-1), and cuminaldehyde (18.39%) (IUPAC: 4-propan-2-ylbenzaldehyde; CAS No. 122-03-2), which were identified as the major constituents of the essential oil (Table 1). These compounds have consistently been reported as the principal volatile constituents of *C. cyminum* essential oil collected from different geographical regions and are considered important contributors to its biological activity (Chen *et al*., 2011).

Cuminaldehyde has been widely reported to possess insecticidal, fumigant, repellent, and antioxidant activities against several stored-product insect pests, while γ-terpinen-7-al (p-mentha-1,4-dien-7-al) has also been identified as a major bioactive aldehyde of cumin

essential oil that contributes to its insecticidal efficacy. Therefore, these compounds are likely to play a key role in the biological performance of the developed active films (Nouri *et al*., 2024).

The essential oil was successfully incorporated into stable nanoemulsions using an ultrasonic emulsification process. Dynamic light scattering (DLS) analysis revealed that the 0.25% *C. cyminum* nanoemulsion exhibited a unimodal droplet size distribution (Fig. 1), with the smallest mean droplet diameter (47.94 nm) and a low polydispersity index (PDI = 0.23), indicating a narrow particle size distribution and excellent homogeneity (Table 2). Such a low PDI value reflects the formation of a highly uniform nanoemulsion with desirable colloidal characteristics. The remarkable physical stability of the nanoemulsions can be primarily attributed to the steric stabilization provided by the nonionic surfactant Tween 80, which effectively prevented droplet aggregation regardless of electrostatic interactions.

**Table 1. Chemical composition of *Cuminum cyminum* essential oil determined by GC–MS.**

| Essential oil | Compounds | Amount (%) |
|---|---|---|
| *C. cyminum* | γ--terpinen-7-al | 30.51 |
| | γ-Terpinene | 18.61 |
| | Cuminaldehyde | 18.39 |
| | β-Pinene | 12.31 |
| | p-Cymene | 5.47 |
| | Other compounds | 14.71 |

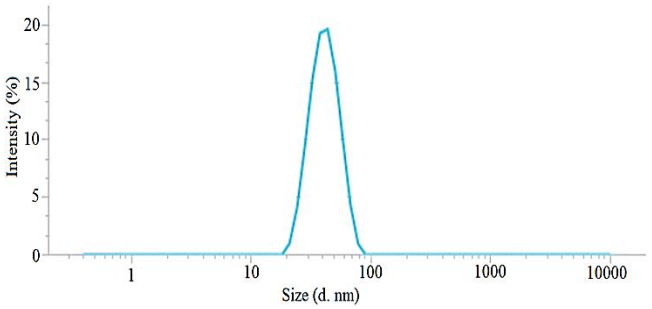



**Figure 1. Intensity-based particle size distribution of the 0.25% *Cuminum cyminum* essential oil nanoemulsion determined by dynamic light scattering (DLS).**

**Table 2. Dynamic light scattering (DLS) characteristics of the 0.25% *Cuminum cyminum* essential oil nanoemulsion**

| Parameter | Value | Unit |
|---|---|---|
| Z-average diameter | 47.94 | nm |
| Polydispersity index (PDI) | 0.230 | - |
| Peak diameter (Intensity) | 22.16-43.45 | nm |

Scanning electron microscopy (SEM) further confirmed the successful incorporation and homogeneous distribution of the nanoemulsion droplets within the WPI/gelatin matrix (Fig. 1). The micrographs revealed a compact and continuous film surface containing uniformly dispersed spherical nanostructures with smooth morphology. Notably, films containing *C. cyminum* nanoemulsion exhibited a denser and more refined microstructure than the control film, which is consistent with the smaller droplet size determined by DLS analysis. SEM observations also demonstrated that spherical nanoemulsion droplets were embedded throughout the protein matrix with no evidence of phase separation or extensive aggregation. Although a slight increase in droplet size was observed at higher nanoemulsion concentrations, the droplets remained relatively homogeneous and well dispersed within the film network, in agreement with the Z-average diameter and PDI values obtained by DLS. This structural integrity indicates that ultrasonic emulsification efficiently stabilized the essential oil droplets within the WPI/gelatin network, thereby promoting the formation of a cohesive and continuous active film. Furthermore, the compact microstructure observed in films containing different concentrations of nanoemulsion suggests that the incorporation of the nanoemulsion did not adversely affect film formation or matrix continuity.

To support the qualitative SEM observations, a preliminary quantitative image analysis was performed using ImageJ software. The equivalent diameter of the clearly distinguishable dispersed domains ranged from approximately 1.03 to 3.95 μm, with an average equivalent diameter of 2.56 ± 1.25 μm (n = 4). These structures represent micrometer-scale oil-rich domains or agglomerates embedded within the WPI/gelatin matrix, rather than the primary nanoemulsion droplets. The actual droplet size was determined by dynamic light scattering (DLS), which showed an average particle diameter of 47.94 nm with a polydispersity index (PDI) of 0.230. Therefore, the SEM observations mainly confirm the homogeneous spatial distribution of the dispersed phase and the compact morphology of the polymer matrix, while the nanoscale droplet size is more accurately represented by the DLS measurements.

Overall, the ultrasound-assisted nanoemulsification technique produced nanoemulsions with narrow particle size distributions and excellent physicochemical stability. The optimum formulation (0.25% *C. cyminum* nanoemulsion) exhibited the

smallest droplet size (47.94 nm) and the lowest PDI, confirming its superior colloidal characteristics. SEM analysis corroborated these findings by revealing dense and homogeneous film matrices without visible phase separation. Even though droplet diameters increased to approximately 100–500 nm in films containing 0.5% nanoemulsion, the droplets remained uniformly distributed throughout the polymer matrix, indicating that the structural integrity of the films was preserved. These findings are in agreement with those reported by Jabbar et al. (2024), who observed particle sizes below 200 nm for ultrasonically prepared *C. cyminum* essential oil nanoemulsions. Similarly, Batista et al. (2024) reported that ultrasonic nanoemulsification produced highly homogeneous nanoemulsions with compact film microstructures and enhanced physical stability, supporting the results obtained in the present study. Although the 0.5% nanoemulsion exhibited superior insecticidal activity in several bioassays, the 0.25% formulation was considered the optimum formulation based on a multi-criteria evaluation rather than biological activity alone. This concentration combined the smallest droplet size (47.94 nm), the lowest polydispersity index (0.230), excellent colloidal stability, homogeneous dispersion within the WPI/gelatin matrix, and favorable mechanical and barrier properties, while still providing strong biological efficacy. Therefore, the selection of the optimum formulation was based on achieving the best overall balance between physicochemical characteristics and insecticidal performance rather than maximizing a single biological endpoint.

### *3.1. Fourier transform infrared (FTIR) spectroscopy and analysis of molecular interactions*

Fourier transform infrared (FTIR) spectroscopy was employed to characterize the chemical structure of the developed nanoemulsions and to investigate the molecular interactions between *C. cyminum* essential oil (CEO) and the WPI/gelatin matrix. As shown in Figs. 2 and 3, the FTIR spectra of the control nanoemulsion and CEO-loaded nanoemulsion exhibited several common absorption bands, confirming that both systems shared the same fundamental structural framework consisting of the aqueous phase and emulsifying agents.

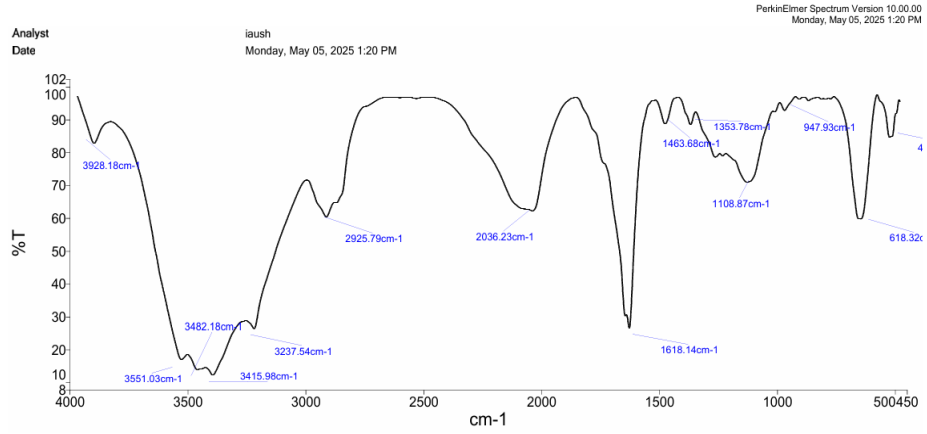



**Figure 2. FTIR spectrum of the blank nanoemulsion (without *Cuminum cyminum* essential oil).**

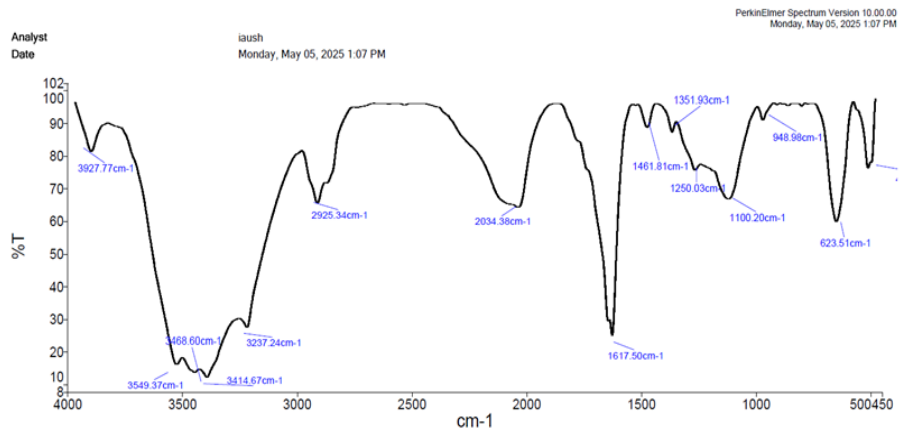



**Figure 3. FTIR spectrum of the blank nanoemulsion of *Cuminum cyminum* essential oil**.

A broad and intense absorption band observed within the range of 3200–3600 $cm^{-1}$ was assigned to O–H stretching vibrations. This band appeared at 3549, 3468, 3414, and 3237 $cm^{-1}$ in the CEO nanoemulsion and at 3551, 3482, 3415, and 3237 $cm^{-1}$ in the control formulation (Figs. 2 and 3). The broadness of this band reflects extensive hydrogen bonding among water molecules, whey protein isolate (WPI), gelatin, and hydroxyl-containing groups of Tween 80, indicating the formation of a highly hydrated and interconnected polymeric network.

Both spectra also displayed characteristic aliphatic C–H stretching vibrations in the region of approximately 2925 $cm^{-1}$, corresponding to the asymmetric stretching of $CH_2$ and $CH_3$ groups originating from the hydrocarbon chains of the surfactant and other organic constituents of the nanoemulsion. In addition, a distinct absorption band at approximately 1618 $cm^{-1}$ was observed in both samples and attributed to C=C stretching vibrations together with contributions from amide I vibrations of the protein matrix, reflecting the structural backbone of the WPI/gelatin network.

The most significant evidence for the successful incorporation of CEO was observed in the fingerprint region (1500–600 $cm^{-1}$). A new characteristic absorption band appeared at 1250.03 $cm^{-1}$ exclusively in the CEO-loaded nanoemulsion, whereas this peak was absent in the control sample. This band can be assigned to C–O stretching vibrations associated with phenolic, ester, and oxygenated terpenoid compounds, particularly cuminaldehyde and other oxygen-containing constituents of *C. cyminum* essential oil. The emergence of this characteristic peak provides direct spectroscopic evidence for the successful encapsulation of CEO within the nanoemulsion system.

Furthermore, the CEO-loaded nanoemulsion exhibited a distinct carbonyl (C=O) stretching band at 1746 $cm^{-1}$, which is characteristic of aldehydic and ester functional groups present in the essential oil. The appearance of this band, together with slight shifts in the hydroxyl and amide absorption regions, suggests the establishment of intermolecular hydrogen bonding between oxygenated compounds of the essential oil and functional groups of WPI and gelatin. These spectral changes indicate that the essential oil was not merely physically dispersed but became molecularly associated with the protein network through non-covalent interactions. Quantitative comparison of the FTIR spectra revealed measurable changes after incorporation of cumin essential oil into the WPI/gelatin matrix. In the broad O–H/N–H stretching region, the absorption band shifted from 3482 $cm^{-1}$ in the control sample to 3468 $cm^{-1}$ in the cumin-containing sample, corresponding to a 14 $cm^{-1}$ shift toward a lower wavenumber. Such a red shift is generally associated with stronger hydrogen-bonding interactions between hydroxyl or amino groups of the polymer matrix and oxygen-containing constituents of cumin essential oil.

Smaller shifts observed in the remaining O–H/N–H stretching bands further support changes in the hydrogen-bonding environment following incorporation of the nanoemulsion. In addition, the appearance of absorption bands at 1746 $cm^{-1}$ and 1250.03 $cm^{-1}$ confirmed the presence of carbonyl- and C–O-containing compounds originating from cumin essential oil within the polymer network.

No evidence for the formation of new covalent bonds was observed. Therefore, the interaction between the encapsulated essential oil and the WPI/gelatin matrix is mainly attributed to non-covalent interactions, including hydrogen bonding, dipole–dipole interactions, and hydrophobic associations. These interactions are considered partially reversible and may be weakened under conditions such as increased moisture or elevated temperature.

The molecular interactions identified by FTIR are also expected to reduce the mobility of volatile essential-oil compounds within the polymer matrix and consequently promote a more gradual diffusion-controlled release. However, because release kinetics were not directly measured in the present study, this proposed mechanism should be regarded as a mechanistic interpretation supported by FTIR evidence rather than direct experimental confirmation.

The optimized CEO nanoemulsion (0.25%) exhibited a mean droplet diameter below 50 nm, indicating excellent colloidal stability and enhanced resistance to Ostwald ripening. According to Nasr Azadani et al. (2025), nanoemulsions within this size range possess improved kinetic stability and can readily penetrate the microscopic pores of the insect cuticle, facilitating transport of bioactive compounds into the hemolymph and thereby enhancing insecticidal efficacy. The FTIR results further demonstrated that

the functional groups of CEO, particularly cuminaldehyde, were effectively retained within the WPI/gelatin matrix through hydrogen-bonding interactions. Similar molecular interactions have been reported by Sheikhi et al. (2025) and Wang et al. (2019), who demonstrated that hydrogen bonding between essential oils and protein-based matrices plays a crucial role in improving encapsulation efficiency, reducing volatility, and enhancing the controlled release of volatile compounds.

These molecular interactions are particularly important because the rapid evaporation and poor environmental stability of essential oils remain major obstacles to their practical application as botanical pesticides. As highlighted by Danna et al. (2024), encapsulation technologies are essential for overcoming these limitations by improving the retention and sustained release of volatile bioactive compounds. Therefore, the observed shifts in the amide and hydroxyl bands, together with the appearance of the new carbonyl and C–O absorption peaks, provide strong evidence for the successful encapsulation of CEO within the WPI/gelatin matrix. This molecular integration is expected to enhance the long-term stability of the active compounds, improve the barrier properties of the films, and enable sustained release of the essential oil, thereby contributing to prolonged insecticidal activity against *S. oryzae*.

### *3.2. Physicochemical and mechanical properties of WPI/gelatin active films*

The incorporation of *C. cyminum* essential oil nanoemulsion significantly influenced the mechanical and barrier properties of the WPI/gelatin active films (Table 3). Overall, increasing the nanoemulsion concentration from 0.10% to 0.25% and subsequently to 0.50% improved the structural integrity of the films while enhancing their resistance to water vapor transmission.

### *3.3. Mechanical properties*

A progressive increase in tensile strength (TS) was observed with increasing nanoemulsion concentration. The TS values increased from 18.00 MPa at 0.10% nanoemulsion to 19.10 MPa at 0.25%, reaching a maximum of 20.10 MPa at 0.50% (Table 3). This improvement indicates that the nanoemulsion droplets acted as nanoscale reinforcing fillers within the WPI/gelatin matrix, promoting stronger intermolecular interactions and improving stress transfer throughout the polymer network. The homogeneous dispersion of the nanoemulsion, confirmed by SEM analysis, likely contributed to the formation of a more compact and mechanically resistant structure.

Elongation at break (EAB) remained relatively high across all formulations, indicating that the incorporation of the nanoemulsion did not compromise film flexibility. The highest EAB value (85.30%) was recorded for the film containing 0.50% nanoemulsion, suggesting that the plasticizing effect of the dispersed oil droplets and the relatively high moisture content (22.10%) compensated for the increased rigidity associated with higher nanoemulsion loading. Consequently, the films simultaneously exhibited enhanced strength and excellent flexibility, properties that are particularly desirable for active packaging applications requiring both mechanical resistance and adaptability during handling. Although the 0.50% formulation produced the highest TS, the film containing 0.25% nanoemulsion provided the most balanced mechanical performance. This concentration achieved sufficient tensile strength (19.10 MPa) while maintaining high flexibility, making it the optimum formulation for rice packaging applications where mechanical durability and flexibility are equally important.

### *3.4. Barrier properties*

Water vapor permeability (WVP) was selected as the principal barrier property because moisture migration is one of the most important factors affecting the quality and storage stability of rice. Excessive moisture facilitates fungal contamination, accelerates physicochemical deterioration, and provides favorable conditions for the development of storage insects such as *S. oryzae*. Therefore, improving the resistance of the edible film to water vapor transmission was considered the most relevant barrier characteristic for the intended application of this study.

Although oxygen permeability and oil resistance are also important barrier properties for certain food-packaging applications, they were beyond the scope of the present work. Rice is a relatively low-lipid cereal, and the primary objective of the developed edible film was to reduce moisture transfer while improving the retention and gradual release of cumin essential oil for

insect control. Consequently, WVP was selected as the most appropriate barrier parameter for evaluating the protective performance of the active film under rice storage conditions.

Future studies will investigate oxygen permeability, carbon dioxide permeability, and oil resistance to provide a more comprehensive evaluation of the barrier performance of the developed edible films for grain-packaging applications.

Increasing the nanoemulsion concentration markedly improved the water vapor barrier performance of the films. Water vapor permeability (WVP) gradually decreased from 0.98 to 0.92 and finally to 0.85 with increasing CEO nanoemulsion concentration (Table 3). This reduction demonstrates that the hydrophobic oil droplets effectively hindered moisture diffusion through the polymer matrix. The dispersed nanoemulsion droplets created a more tortuous diffusion pathway for water molecules, thereby reducing water vapor transmission.

The decrease in WVP can be explained by the tortuous path theory, whereby uniformly distributed hydrophobic nanoparticles increase the diffusion distance that water molecules must travel through the film matrix. Similar mechanisms have been reported by Ji et al. (2026) and Tan et al. (2019), who demonstrated that essential oil nanoemulsions act as nanoscale fillers occupying intermolecular voids within biopolymer networks, thereby improving moisture barrier properties and reinforcing the polymer structure. Water solubility (WS) showed only a slight increase with increasing nanoemulsion concentration, rising from 14.50% to 15.00% and finally to 15.60%. This modest increase may be attributed to structural rearrangements within the polymer network induced by the higher essential oil content. Nevertheless, the increase was relatively small, indicating that the films retained satisfactory water resistance despite the incorporation of increasing amounts of nanoemulsion. Among the tested formulations, the film containing 0.25% CEO nanoemulsion represented the optimal balance between mechanical performance and barrier functionality. Compared with the 0.10% formulation, this concentration significantly reduced water vapor permeability while preserving desirable tensile strength and flexibility. Although the 0.50% film exhibited the lowest WVP and the highest TS, the improvements over the 0.25% formulation were comparatively limited, suggesting that 0.25% is sufficient to achieve an effective balance between mechanical reinforcement and moisture barrier performance.

The enhanced physicochemical properties observed in the CEO-loaded films are closely associated with the formation of a denser polymeric network, as evidenced by SEM and FTIR analyses. The homogeneous distribution of nanoemulsion droplets reduced intermolecular free volume, strengthened intermolecular interactions, and generated an efficient physical barrier against water vapor diffusion. Similar improvements in tensile strength, elongation at break, and moisture barrier properties have been reported for protein-based nanocomposite films containing essential oil nanoemulsions by Lozano-Navarro et al. (2017) and Atarés and Chiralt (2016). Furthermore, the formation of this compact network is expected to enhance the long-term stability of the encapsulated bioactive compounds by limiting their rapid diffusion and evaporation, thereby contributing to sustained insecticidal activity during storage.

**Table 3. Physicochemical and mechanical properties of WPI/gelatin active films incorporated with *Cuminum cyminum* essential oil nanoemulsion.**

| Property | *C. cyminum* concentration | | |
|---|---|---|---|
| | 0.1 | 0.25 | 0.5 |
| Tensile strength (TS, MPa) | 18 | 19.10 | 20.10 |
| Elongation at break (EAB, %) | 87.50 | 86.80 | 85.30 |
| Water vapor permeability | 0.98 | 0.92 | 0.85 |
| Moisture content (MC %) | 21 | 21.60 | 22.10 |
| Water solubility (WS, %) | 14.50 | 15 | 15.60 |

### *3.5. Repellent activity of WPI/gelatin active films*

The repellent activity of WPI/gelatin active films incorporated with *C. cyminum* essential oil (CEO) nanoemulsion increased in a concentration-dependent manner against both larval and adult stages of *S. oryzae* (Table 4). Overall, CEO-loaded films exhibited significantly greater repellency at higher nanoemulsion concentrations, indicating that increasing the amount of encapsulated essential oil enhanced the release of volatile bioactive compounds responsible for insect avoidance.

Among the tested formulations, the highest repellency index (RI) against larvae was achieved by the film containing 0.25% CEO nanoemulsion (RI = 0.87), whereas the strongest repellent effect against adults was observed with the 0.50% formulation (RI = 0.76). These findings indicate that larvae were more

sensitive to CEO volatiles than adults, reaching maximum repellency at a lower nanoemulsion concentration. In contrast, adult insects required a higher concentration to achieve a comparable behavioral response, possibly due to differences in olfactory sensitivity, cuticular permeability, and physiological tolerance.

Both the 0.25% and 0.5% CEO nanoemulsion films exhibited high repellency against *S. oryzae*. Although the 0.5% treatment showed a numerically higher repellency index, no statistically significant difference was observed between the two treatments (P>0.05), as indicated by their shared statistical grouping in Table 4.

**Table 4. Pairwise comparison of the repellency index (RI) in larval and adult *Sitophilus oryzae*.**

| Treatment | Mean larval repellency index (RI) | Mean adult insect repellency index (RI) |
|---|---|---|
| Control | -0.02$^{d}$ | -0.15$^{e}$ |
| C. *cyminum* (0.1) | 0.45$^{b}$ | 0.43$^{c}$ |
| C. *cyminum* (0.25) | 0.87$^{a}$ | 0.80$^{a}$ |
| C. *cyminum* (0.5) | 0.77$^{a}$ | 0.76$^{a}$ |

Means sharing at least one same letter do not differ significantly according to Duncan's multiple range test (p≤0.05)

Although the repellency generally increased with increasing CEO concentration, a slight decrease in the larval repellency index was observed at the highest concentration (0.5% CEO) compared with the 0.25% treatment. Such a non-monotonic response has occasionally been reported for volatile plant-derived compounds and may reflect complex insect behavioral responses rather than a simple dose-dependent effect. One possible explanation is temporary adaptation or partial saturation of olfactory receptors after exposure to elevated concentrations of volatile compounds. Another possibility is that increasing the essential-oil loading modifies its release behavior from the WPI/gelatin matrix through stronger molecular interactions, thereby changing the concentration of volatile compounds available during the bioassay. Overstimulation by high volatile concentrations may also contribute to altered behavioral responses. Since volatile release profiles and release kinetics were not determined in the present study, these explanations should be considered as mechanistic hypotheses. Future investigations combining volatile-release analysis with behavioral bioassays will be valuable for clarifying this phenomenon. The observed non-monotonic repellency response also highlights that increasing the concentration of an essential oil does not necessarily result in proportionally greater biological activity. The effectiveness of active packaging systems depends not only on the amount of essential oil incorporated into the film but also on its release dynamics and the behavioral sensitivity of the target insect.

### *3.6. Fumigant toxicity and probit analysis*

The fumigant bioassay and probit analysis demonstrated significant differences in the susceptibility of the developmental stages of *S. oryzae* to the WPI/gelatin active films containing *C. cyminum* essential oil (CEO) nanoemulsion. Based on the median lethal concentration ($LC_{50}$) values (Table 5), larvae were considerably more susceptible than adult insects, indicating that the efficacy of the active films was strongly influenced by the insect developmental stage. Among all formulations, the film containing 0.50% CEO nanoemulsion exhibited the greatest fumigant toxicity against larvae, with the lowest $LC_{50}$ value of 0.559 μL $L^{-1}$, demonstrating its superior insecticidal potency. In contrast, adult insects required higher concentrations to achieve comparable mortality, reflecting their greater physiological tolerance.

**Table 5. Probit analysis parameters for lethal concentration (LC) and lethal time (LT) of WPI/gelatin active films containing *Cuminum cyminum* essential oil nanoemulsion against *Sitophilus oryzae*.**

| Treatment | Life stage | $LC_{50}$ (μL $L^{-1}$), (95% CI) | $LC_{90}$ (μL $L^{-1}$) | Slope (time) | $X^2$ (df=1) | p-value | $LT_{50}$ (h), (95% CI) | $LT_{90}$ (h) | Slope (time) | $X^2$ (df=5) | p-value |
|---|---|---|---|---|---|---|---|---|---|---|---|
| Nanoemulsion (*C. cyminum*) | Adult | 1.178 (0.362-3.839) | 20.383 | 1.035 | 1.627 | 0.202$^{ns}$ | 48.634 (38.75-60.96) | 181.935 | 2.237 | 0.564 | 0.99$^{ns}$ |
| | Larval | 0.559 (0.310-1.010) | 6.325 | 1.216 | 2.631 | 0.105$^{ns}$ | 46.540 (38.03-56.90) | 155.52 | 2.446 | 0.532 | 0.991$^{ns}$ |

The enhanced susceptibility of larvae may be attributed to their thinner and less sclerotized cuticle, higher respiratory activity, and greater permeability to volatile compounds, allowing more efficient penetration of the bioactive constituents into the insect body. The concentration–mortality relationships obtained from probit analysis revealed a strong linear association between the logarithm of CEO concentration and larval mortality (Fig. 4; Table 5). The close agreement between the experimental

observations and the fitted regression lines confirms the robustness of the probit model and indicates a predictable dose-dependent toxic response. Such linearity suggests that increasing CEO concentration consistently enhanced fumigant toxicity, supporting the reliability of the estimated lethal concentrations.

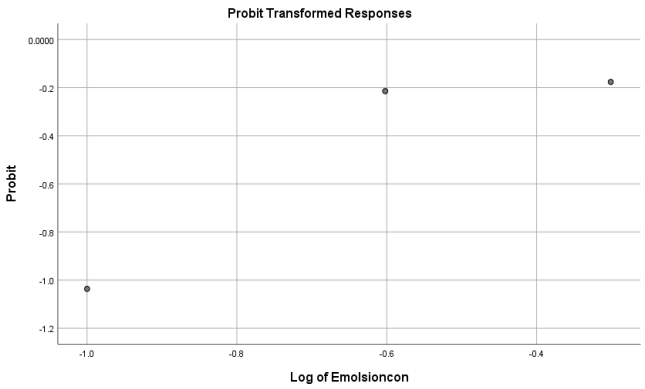



**Figure 4. Probit-transformed concentration–mortality response of *Sitophilus oryzae* larvae exposed to WPI/gelatin active films containing *Cuminum cyminum* essential oil nanoemulsion.**

The $LC_{50}$ value of 0.559 µL $L^{-1}$ air obtained against *S. oryzae* larvae demonstrates the remarkable fumigant efficacy of the developed active film. Compared with recently reported essential oil nanoemulsions, which exhibited fumigant $LC_{50}$ values ranging from 14.3 to 17.9 µL $L^{-1}$ air against stored-product insects, the present formulation showed substantially greater potency, highlighting the effectiveness of incorporating cumin essential oil nanoemulsion into the WPI/gelatin matrix (Jasman *et al.*, 2025) Although phosphine remains one of the most effective commercial fumigants due to its high intrinsic toxicity, its long-term application has resulted in widespread resistance among stored-product insects, concerns regarding chemical residues, and environmental and occupational safety issues. Essential oil-based active films represent an environmentally friendly alternative by providing sustained release of volatile bioactive compounds, reducing reliance on synthetic fumigants while minimizing ecological impacts (Kannan and Chandrasekaran, 2026).

Based on the experimental configuration used in this study (a 2 × 1 cm active film in a 200 mL chamber), approximately 25–30 $cm^2$ of active film per kilogram of rice is theoretically estimated to achieve a fumigant concentration comparable to the $LC_{50}$ under closed-storage conditions. This estimation is intended as a practical guideline and may vary depending on storage conditions, package geometry, headspace volume, temperature, and the release behavior of the essential oil (Wang *et al.*, 2026)

The $LT_{50}$ value was estimated by probit analysis using the complete time–mortality dataset. Therefore, the estimated $LT_{50}$ of 46.54 h is consistent with the observed larval mortality of 87.50% at 48 h, reflecting the continued increase in mortality beyond the median lethal time. The time–mortality analysis further demonstrated that the 0.50% CEO nanoemulsion film was the most rapidly acting treatment against larvae, producing the shortest median lethal time ($LT_{50}$ = 46.54 h). This formulation achieved 50% larval mortality more rapidly than all other treatments, indicating a faster onset of toxic action. The superior performance of the 0.50% formulation was also visually confirmed by the time–mortality curves (Fig. 5), in which this treatment reached the mortality thresholds substantially earlier than films containing lower nanoemulsion concentrations.

Consistent with these findings, cumulative mortality data (Table 6) showed that after 48 h of exposure, the 0.50% CEO nanoemulsion film produced the highest mortality in both larval and adult populations. Although mortality increased with nanoemulsion concentration in both life stages, larvae consistently exhibited greater susceptibility throughout the experimental period. The probit slope values also provided valuable information regarding population homogeneity and toxicological response. The highest slope value (1.216) was obtained for larvae exposed to the 0.50% CEO nanoemulsion (Table 5), indicating a steeper dose–response relationship and a more uniform susceptibility of the larval population to increasing CEO concentrations.

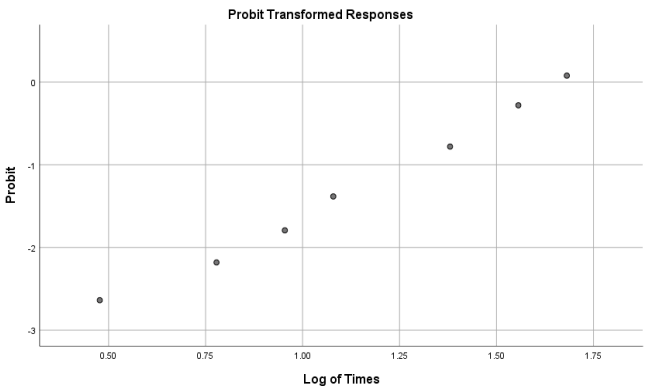



**Figure 5. Probit-transformed time–mortality response of *Sitophilus oryzae* larvae exposed to WPI/gelatin active films containing *Cuminum cyminum* essential oil nanoemulsion.**

**Table 6. Pairwise comparison of the mean fumigant toxicity at different exposure times in larval and adult *Sitophilus oryzae***

| Treatment | | 3h | 6h | 9h | 12h | 24h | 36h | 48h |
|---|---|---|---|---|---|---|---|---|
| Larval | Control | $0^{b}$ | $0^{b}$ | $0^{c}$ | $0.42^{e}$ | $1.25^{e}$ | $1.67^{d}$ | $2.50^{e}$ |
| | 0.1 *C. cyminum* | $0^{b}$ | $0^{b}$ | $1.67^{c}$ | $5.83^{d}$ | $11.25^{d}$ | $23.75^{c}$ | $32.50^{d}$ |
| | 0.25 *C. cyminum* | $0.83^{b}$ | $6.92^{a}$ | $6.25^{b}$ | $13.33^{c}$ | $35^{c}$ | $62.92^{b}$ | $90.00^{a}$ |
| | 0.5 *C. cyminum* | $0.83^{b}$ | $6.92^{a}$ | $6.67^{b}$ | $13.75^{c}$ | $39.58^{a}$ | $67.50^{a}$ | $87.50^{b}$ |
| Adult | 0.1 *C. cyminum* | $0^{b}$ | $0.42^{c}$ | $1.67^{c}$ | $5^{d}$ | $12.08^{d}$ | $25.83^{c}$ | $32.92^{d}$ |
| | 0.25 *C. cyminum* | $1.25^{a}$ | $2.92^{b}$ | $10^{a}$ | $15^{b}$ | $36.25^{bc}$ | $63.75^{ab}$ | $80.83^{c}$ |
| | 0.5 *C. cyminum* | $1.25^{a}$ | $3.33^{ab}$ | $9.17^{ab}$ | $17.50^{a}$ | $37.50^{b}$ | $67.08^{a}$ | $85.42^{b}$ |

### *3.7. Larval penetration assay*

The larval penetration assay demonstrated that the WPI/gelatin active films significantly inhibited the penetration of *S. oryzae* larvae compared with the control treatment ($P<0.001$). The 21-day evaluation period (Table 7) revealed that increasing the concentration of *C. cyminum* essential oil (CEO) nanoemulsion within the polymer matrix progressively enhanced the barrier performance of the films, indicating a clear concentration-dependent protective effect. Among the tested formulations, the film containing 0.50% CEO nanoemulsion exhibited the highest resistance to larval penetration, limiting penetration to only 24.16% after 21 days of storage (Table 7). This substantial reduction demonstrates that the active film functioned not only as a physical barrier but also as a chemically active packaging material capable of deterring or suppressing larval movement through continuous release of insecticidal volatiles.

The incomplete larval penetration observed in the control film suggests that the WPI/gelatin matrix itself may provide a partial physical barrier against larval penetration. However, the incorporation of cumin essential oil nanoemulsion markedly enhanced this protective effect, resulting in significantly lower penetration rates compared with the control film.

**Table 7. Larval penetration (%) of *Sitophilus oryzae* through WPI/gelatin active films containing *Cuminum cyminum* essential oil nanoemulsion during 21 days of storage.**

| Treatment | Conc.(%) | 7 days | 14 days | 21 days |
|---|---|---|---|---|
| Control | - | $24.16\pm2.48^{a}$ | $50.00\pm1.98^{a}$ | $68.75\pm2.98^{a}$ |
| Nanoemulsions *C. cyminum* | 0.1 | $15.00\pm2.48^{b}$ | $31.66\pm1.98^{b}$ | $50.00\pm2.98^{c}$ |
| | 0.25 | $11.66\pm2.48^{c}$ | $20.83\pm1.98^{c}$ | $33.75\pm2.98^{d}$ |
| | 0.5 | $6.66\pm2.48^{d}$ | $14.16\pm1.98^{e}$ | $24.16\pm2.98^{e}$ |

### *3.8. Relationship between fumigant toxicity, repellency, and biochemical responses*

The WPI/gelatin active film containing 0.50% *C. cyminum* essential oil (CEO) nanoemulsion exhibited the greatest insecticidal efficacy, with an $LC_{50}$ of 0.559 μL $L^{-1}$ air and an $LT_{50}$ of 46.54 h, while the highest repellency against larvae was obtained with the 0.25% formulation (RI = 0.87). These results indicate that the CEO nanoemulsion provided both rapid fumigant activity and strong behavioral deterrence against *S. oryzae*.

The differences observed in $LT_{50}$ values are likely associated with the volatility and vapor pressure of the major volatile constituents of CEO. Oxygenated monoterpenoids and aromatic aldehydes with relatively low molecular weights readily evaporate and diffuse through the insect respiratory system, thereby accelerating fumigant activity. This interpretation is consistent with the findings of Bakkali et al. (2008) and Jesser et al. (2022), who demonstrated that the insecticidal performance of essential oils is strongly influenced by the physicochemical properties of their volatile constituents.

Furthermore, the relatively steep probit slope obtained for the CEO nanoemulsion indicates a homogeneous toxic response of the insect population to increasing concentrations. According to the classical probit approach of Miller and Tainter (1944), steeper slopes reflect lower variability in susceptibility among individuals and a more consistent toxic effect across the exposed population. The high biological activity observed in the present study is likely related to the predominance of cuminaldehyde, which was identified by GC–MS as one of the principal constituents of CEO. Cuminaldehyde has been widely reported to possess strong insecticidal and repellent properties because of its high lipophilicity and its ability to readily penetrate insect tissues. Compared with many hydrocarbon monoterpenes, aromatic aldehydes generally exhibit greater chemical stability and prolonged biological activity, which may contribute to the sustained toxicity observed in the nanoemulsion films.

In addition to cuminaldehyde, other monoterpenes present in CEO, including β-pinene and γ-terpinene, may contribute synergistically to the overall insecticidal activity. Such synergistic interactions

among essential oil constituents have frequently been reported to enhance fumigant toxicity and repellency beyond the activity of individual compounds. Similar observations have been reported by Msegued Ayam et al. (2025), who demonstrated that *C. cyminum* essential oil exhibits potent repellent and insecticidal activities against stored-product pests through the combined action of multiple terpenoid constituents. The strong repellency exhibited by the CEO-loaded films suggests that continuous release of volatile compounds generated an effective olfactory barrier, preventing insects from approaching or colonizing the packaged commodity. Simultaneously, insects that remained exposed to these volatiles experienced pronounced physiological stress, resulting in increased mortality and reduced penetration ability. Therefore, the active films function through complementary mechanisms, acting both as a physical barrier provided by the compact WPI/gelatin matrix and as a functional chemical barrier through the sustained release of volatile bioactive compounds. This dual mode of action explains the marked reduction in larval penetration observed during storage.

### *3.9. Biochemical responses*

To further elucidate the mode of action of the CEO nanoemulsion, the activities of key detoxification and neurophysiological enzymes, including esterases, glutathione S-transferase (GST), and acetylcholinesterase (AChE), were evaluated following exposure to the most effective CEO nanoemulsion concentrations (0.25% and 0.50%). Enzyme activities were expressed as specific activity (U $mg^{-1}$ protein) to normalize variations in total protein content. Biochemical analyses were performed under three experimental conditions: E1, fumigant toxicity against larvae; E2, fumigant toxicity against adults; and E3, larval penetration assay. Based on the untreated controls, enzyme activities within the range of 380–440 U $mg^{-1}$ protein were considered representative of normal physiological levels (Table 8; Fig. 6).

**Table 8. Percentage of normal AChE, GST, and esterase activities in *Sitophilus oryzae* following different active film treatments**

| Treatment | ACHE (%Active) | GST (%Active) | Esterase (%Active) |
|---|---|---|---|
| Control | 66.7 | 100 | 33.3 |
| 0.25 *C. cyminum* | 33.3 | 0 | 66.7 |
| 0.5 *C. cyminum* | 66.7 | 33.3 | 33.3 |

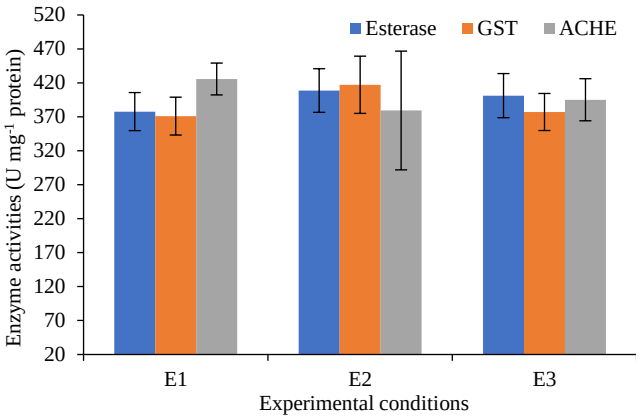



**Figure 6. Mean activities of neurophysiological and detoxification enzymes in *Sitophilus oryzae* under different exposure scenarios. E1, larval fumigant toxicity assay; E2, adult fumigant toxicity assay; and E3, larval penetration assay. Enzyme activities are expressed as mean ± SD (U $mg^{-1}$ protein).**

### *3.10. Biochemical responses and correlation analysis*

#### *3.10.1. Acetylcholinesterase (AChE)*

Acetylcholinesterase (AChE), a key enzyme responsible for terminating nerve impulse transmission, was evaluated as the principal biomarker of neurotoxicity induced by the CEO nanoemulsion-based active films. The results demonstrated that the neurophysiological response of *S. oryzae* was strongly influenced by both developmental stage and exposure scenario (Tables 8 and 9).

**Table 9. Mean enzyme activities (mean ± SD) of *Sitophilus oryzae* under different experimental conditions.**

| Experimental conditions | Esterase (Mean±SD) | GST (Mean±SD) | ACHE (Mean±SD) |
|---|---|---|---|
| Larval fumigant toxicity | 337.7±28.04 | 371.1±27.88 | 425.7±23.51 |
| Adult fumigant toxicity | 408.7±32.10 | 417.2±42.15 | 379.3±87.47 |
| Larval penetration | 401.2±32.48 | 377.1±27.27 | 395.1±31.00 |

The normal range of enzyme activity was defined as 380–440 U $mg^{-1}$ protein.

The greatest inhibition of AChE activity was observed in fumigant-exposed adults (E2), where the mean enzyme activity decreased to 379.3 U $mg^{-1}$ protein, falling below the normal physiological range (380–440 U $mg^{-1}$ protein). This pronounced reduction indicates that volatile compounds released from the CEO nanoemulsion films effectively interfered with cholinergic neurotransmission in adult insects, resulting in stronger neurotoxic effects during fumigation. Because enzyme activity was expressed as specific activity (U $mg^{-1}$ protein), the observed inhibition reflects a genuine reduction in enzymatic function rather than differences in total protein content.

In contrast, larval insects exhibited a more moderate neurophysiological response. During the larval

fumigation assay (E1), AChE activity remained within the normal physiological range, with a mean value of 425.7 U $mg^{-1}$ protein, suggesting greater tolerance or lower susceptibility of the larval nervous system under these exposure conditions. In the larval penetration assay (E3), enzyme activity declined to 395.1 U $mg^{-1}$ protein, indicating moderate inhibition during prolonged contact with the active films (Table 9).

Among the tested formulations, the 0.25% CEO nanoemulsion film produced the strongest inhibitory effect on AChE, with only 33.3% of the exposed insects maintaining normal enzyme activity (Table 8). These findings suggest that the controlled release of CEO constituents from the optimized nanoemulsion was sufficient to induce substantial neurophysiological disruption without requiring the highest essential oil concentration.

*3.10.2. Esterase activity*

Compared with GST and AChE, esterase activity was less affected by exposure to the active films, indicating that this detoxification pathway was relatively resistant to CEO nanoemulsion treatment. In insects exposed to the 0.25% CEO nanoemulsion, esterase activity remained within the normal range in all evaluated samples, whereas exposure to the 0.50% formulation reduced the proportion of insects exhibiting normal esterase activity to 33.3% (Table 8). These findings suggest that increasing CEO concentration progressively impaired esterase-mediated detoxification, although the effect remained less pronounced than that observed for GST.

*3.10.3. Glutathione S-transferase (GST)*

Among all biochemical biomarkers evaluated, glutathione S-transferase (GST) was the most sensitive to CEO nanoemulsion exposure. Complete suppression of normal GST activity was observed in insects treated with the 0.25% CEO nanoemulsion, with no individuals (0%) exhibiting enzyme activity within the physiological range. Furthermore, during the larval fumigation assay (E1), mean GST activity decreased to 371.1 U $mg^{-1}$ protein, indicating severe impairment of the insect detoxification system (Tables 8 and 9; Fig. 6).

GST plays a central role in Phase II detoxification by catalyzing the conjugation of glutathione with xenobiotic compounds, thereby facilitating their elimination. Consequently, suppression of GST activity suggests a marked reduction in the insect's capacity to detoxify reactive metabolites generated following exposure to CEO volatiles.

*3.11. Correlation analysis*

Correlation analysis revealed a moderate negative correlation between esterase and AChE activities ($r = -0.43$), indicating that reduced esterase activity was associated with greater inhibition of neural function (Table 10). In contrast, GST and AChE exhibited an almost negligible correlation ($r = 0.04$), suggesting that detoxification impairment and neurotoxicity were largely independent physiological responses induced by the active films.

**Table 10. Pearson correlation matrix of the enzyme activities measured in *Sitophilus oryzae***

| Enzyme | Esterase | GST | AChE |
|---|---|---|---|
| Esterase | 1.00 | -0.19 | -0.43 |
| GST | -0.19 | 1.00 | 0.04 |
| AChE | -0.43 | 0.04 | 1.00 |

The marked suppression of GST activity observed in the present study indicates substantial disruption of the insect antioxidant and detoxification systems. According to Jasman et al. (2025), inhibition of GST compromises the insect's ability to conjugate toxic metabolites and neutralize reactive oxygen species, ultimately leading to oxidative stress and increased mortality. Likewise, the reduction in AChE activity, determined using the Ellman et al. (1961) method, supports the occurrence of neurophysiological disruption following exposure to CEO nanoemulsion films. Although the mode of action differs from that of synthetic organophosphate insecticides, inhibition of AChE similarly interferes with cholinergic neurotransmission, contributing to paralysis and insect mortality. Comparable biochemical responses have been reported by Abdelaal et al. (2021), who demonstrated that nanoemulsions prepared from basil and cumin essential oils significantly reduced AChE and β-esterase activities while altering GST activity in stored-product insects. These observations support the hypothesis that nanoencapsulation enhances the interaction between essential oil constituents and critical detoxification and neural enzymes, thereby increasing insecticidal efficacy.

Collectively, the biochemical evidence suggests that the superior performance of the CEO nanoemulsion films results from multiple complementary

mechanisms, including sustained release of volatile bioactive compounds, disruption of cholinergic neurotransmission through AChE inhibition, and impairment of detoxification pathways via GST suppression. The combination of these mechanisms likely explains the enhanced fumigant toxicity, strong repellency, and reduced larval penetration observed throughout the study.

To the best of our knowledge, this is the first study to demonstrate that protein-based active films containing *C. cyminum* essential oil nanoemulsion simultaneously target two complementary physiological pathways in *S. oryzae*: neurotoxicity through AChE inhibition and detoxification failure through GST suppression. This dual mode of action, combined with the controlled-release properties of the WPI/gelatin matrix, highlights the potential of these films as multifunctional active packaging materials for sustainable management of stored-product pests. Despite these promising findings, the present study has some limitations. The long-term stability of the active films and their insecticidal performance under commercial grain-storage conditions were not evaluated. Future studies should investigate release kinetics during prolonged storage, efficacy under fluctuating environmental conditions, and large-scale validation to facilitate practical application. From a food safety perspective, *C. cyminum* essential oil is classified as Generally Recognized as Safe (GRAS) by the U.S. Food and Drug Administration (FDA). Recent toxicological studies have further demonstrated that CEO nanoemulsions exhibit high biocompatibility and no significant adverse biological effects at concentrations effective for pest management (Jabbar *et al*., 2024; Msegued Ayam *et al*., 2025). These characteristics support the potential application of the developed WPI/gelatin active films as safe and environmentally friendly materials for active food packaging and stored-grain protection.

Although the biochemical assays clearly demonstrated concentration-dependent changes in acetylcholinesterase (AChE) and glutathione S-transferase (GST) activities following exposure to CEO-containing edible films, standard positive inhibitors such as eserine (for AChE) and ethacrynic acid (for GST) were not included in the present study. Consequently, the results should be interpreted as relative comparisons among the experimental treatments rather than as direct measurements of inhibitory potency relative to established reference compounds. Future studies incorporating these standard inhibitors will provide additional validation of assay sensitivity and allow direct benchmarking of CEO-induced enzyme modulation against well-characterized biochemical inhibitors.

The correlation analysis suggests that the biochemical responses induced by CEO were not uniformly coordinated among the investigated enzymes. The negligible correlation between GST and AChE ($r = 0.04$) indicates that these enzymes likely responded through largely independent physiological pathways, reflecting their distinct biological roles in detoxification and neurotransmission, respectively. In contrast, the moderate negative correlation between esterase and AChE ($r = -0.43$) may reflect a more complex adaptive response. One possible explanation is a compensatory mechanism, whereby changes in esterase activity partially offset alterations in cholinergic function following exposure to CEO. Alternatively, both enzymes may be influenced by partially overlapping regulatory pathways that respond differently to the bioactive constituents of cumin essential oil. Since molecular regulatory mechanisms were not investigated in the present study, these interpretations should be considered as biologically plausible hypotheses. Future studies integrating enzyme activity measurements with gene-expression or proteomic analyses would provide a deeper understanding of the relationships among these biochemical pathways.

Enzyme activities were evaluated at a single standardized endpoint of 24 h post-exposure. Therefore, the present biochemical results describe the enzymatic status of the insects at this specific time point and do not establish whether the observed changes developed progressively, were reversible, or were followed by physiological recovery. The absence of measurements at earlier and later intervals represents a limitation of the study. Future time-course experiments incorporating multiple sampling points, such as 6, 12, 24, and 48 h, are required to distinguish transient enzyme modulation from persistent biochemical effects and to provide a more detailed mechanistic interpretation of CEO exposure.

Although the physicochemical properties and biological performance of the CEO-containing films

were evaluated separately in the present study, the overall findings suggest a qualitative relationship between film structure and insecticidal efficacy. Films exhibiting lower water vapor permeability and improved mechanical integrity are expected to retain volatile bioactive compounds more effectively and to promote their sustained availability during storage, thereby enhancing insecticidal performance. Nevertheless, no formal Pearson or Spearman correlation analysis was performed between physicochemical parameters and biological endpoints. Future studies based on larger datasets should incorporate correlation and regression analyses to identify the film properties that most strongly predict biological efficacy and to support the development of predictive active-packaging models.

## 4. Conclusion

The present study successfully developed biodegradable WPI/gelatin-based active films incorporating *C. cyminum* essential oil (CEO) nanoemulsion and demonstrated their multifunctional potential for the protection of stored grains against *S. oryzae*. The optimized CEO nanoemulsion exhibited excellent colloidal stability (47.94 nm, PDI = 0.23), while SEM and FTIR analyses confirmed its homogeneous distribution and successful incorporation into the polymeric matrix, resulting in compact films with enhanced mechanical strength and improved water vapor barrier properties. Nanoemulsion incorporation increased tensile strength, maintained high flexibility, and reduced water vapor permeability, indicating effective reinforcement of the WPI/gelatin network. Among the tested formulations, the 0.25% CEO nanoemulsion provided the best balance between physicochemical characteristics and biological performance, whereas the 0.50% formulation exhibited the highest fumigant toxicity and barrier efficiency. Biological assays revealed strong insecticidal activity, with the 0.50% CEO film producing the lowest $LC_{50}$ (0.559 μL $L^{-1}$ air) and $LT_{50}$ (46.54 h) values against larvae, while the 0.25% formulation achieved the highest repellency index (RI = 0.87). Furthermore, larval penetration was reduced to 24.16% after 21 days, confirming prolonged protective activity during storage. Biochemical analyses demonstrated that CEO nanoemulsion disrupted both detoxification and neural pathways through complete GST suppression and significant AChE inhibition, providing a dual biochemical mode of action. Collectively, the combination of controlled release, physical barrier properties, repellency, fumigant toxicity, and enzyme inhibition highlights the superiority of CEO nanoemulsion-loaded films over conventional botanical formulations. To the best of our knowledge, this is the first report demonstrating that protein-based active films containing *C. cyminum* nanoemulsion simultaneously provide sustained repellency, fumigant toxicity, long-term barrier protection, and dual GST/AChE interference against *S. oryzae*. These findings support the application of CEO nanoemulsion-based active packaging as a sustainable alternative to synthetic insecticides and petroleum-based packaging for integrated stored-grain pest management. Nevertheless, additional studies under commercial storage conditions are required to evaluate long-term stability, release kinetics, and large-scale applicability of these biodegradable active films.

### Conflict of interests

All authors declare no conflict of interest.

### Ethics approval and consent to participate

No humans or animals were used in the present research. The authors have adhered to ethical standards, including avoiding plagiarism, data fabrication, and double publication.

### Consent for publications

All authors read and approved the final manuscript for publication.

### Availability of data and material

All the data are embedded in the manuscript.

### Authors' contributions

All authors had an equal role in study design, work, statistical analysis and manuscript writing.

### Informed consent

The authors declare not to use any patients in this research.

### Use of artificial intelligence tools

Some sentences in this manuscript were revised with the assistance of artificial intelligence, using language

models to improve clarity and readability. All intellectual content, interpretations, and conclusions are solely the responsibility of the authors.

## Funding/Support

This research did not receive any specific grant from funding agencies in the public, commercial, or not-for-profit sectors.

## Acknowledgement

The authors would like to thank the Department of Plant Protection, Faculty of Agriculture, Islamic Azad University, Isfahan Branch, for providing laboratory facilities and technical support.

## References

Abdelaal K., Essawy M., Quraytam A., Abdallah F., Mostafa H., Shoueir K., Fouad H., Hassan F.A.S., Hafez Y. 2021. Toxicity of essential oils nanoemulsion against *Aphis craccivora* and their inhibitory activity on insect enzymes. Processes 9(4): 624. https://doi.org/10.3390/pr9040624

Açıkgöz M.A. 2020. Establishment of cell suspension cultures of *Ocimum basilicum* L. and enhanced production of pharmaceutical active ingredients. Industrial Crops and Products 148: 112278. https://doi.org/10.1016/j.indcrop.2020.112278

Adak T., Barik N., Patil N.B., Govindharaj G.P.P., Gadratagi G.B., Annamalai M., Mukherjee A.K., Rath P.C. 2020. Nanoemulsion of eucalyptus oil: An alternative to synthetic pesticides against two major storage insects (*Sitophilus oryzae* (L.) and *Tribolium castaneum* (Herbst)) of rice. Industrial Crops and Products 143: 111849. https://doi.org/10.1016/j.indcrop.2019.111849

Adams R.P. 2007. Identification of essential oil components by gas chromatography/mass spectrometry. 4th ed. Allured Publishing Corporation.

Aghajani F., Rafati H., Aliahmadi A., Moghimi R. 2024. Novel nanoemulsion-loaded hydroxyl propyl methyl cellulose films as bioactive food packaging materials containing *Satureja khuzestanica* essential oil. Carbohydrate Polymer Technologies and Applications 8: 100544. https://doi.org/10.1016/j.carpta.2024.100544

Aider M. 2010. Chitosan application for active bio-based films production and potential in the food industry: Review. *LWT* - Food Science and Technology 43(6): 837-842. https://doi.org/10.1016/j.lwt.2010.01.021

Ashraf S.A., Siddiqui A.J., Elkhalifa A.E.O., Khan M.I., Patel M., Alreshidi M., Moin A., Singh R., Snoussi M. 2021. Innovations in nanoscience for the sustainable development of food and agriculture with implications on health and environment. Science of the Total Environment 768: 144990. https://doi.org/10.1016/j.scitotenv.2021.144990

Atarés L., Chiralt A. 2016. Essential oils as additives in biodegradable films and coatings for active food packaging. Trends in Food Science & Technology 48: 51-62. https://doi.org/10.1016/j.tifs.2015.12.001

Attia M.A., Wahba T.F., Shaarawy N., Moustafa F.I., Guedes R.N.C., Dewer Y. 2020. Stored grain pest prevalence and insecticide resistance in Egyptian populations of the red flour beetle *Tribolium castaneum* (Herbst) and the rice weevil *Sitophilus oryzae* (L.). Journal of Stored Products Research 87: 101611. https://doi.org/10.1016/j.jspr.2020.101611

Bakkali F., Averbeck S., Averbeck D., Idaomar M. 2008. Biological effects of essential oils: A review. Food and Chemical Toxicology 46(2): 446-475. https://doi.org/10.1016/j.fct.2007.09.106

Baqeri Zanouz E. 1999. Principles of insect morphology and physiology. Tehran: University of Tehran Press. 274 p. (In Farsi).

Batista D.G., Sganzerla W.G., da Silva L.R., Vieira Y.G.S., Almeida A.R., Dominguini D., Ceretta L., Pinheiro A.C., Bertoldi F.C., Becker D., Hotza D., Nunes M.R., da Rosa C.G., Masiero A.V. 2024. Antimicrobial and cytotoxic potential of eucalyptus essential oil-based nanoemulsions for mouthwashes application. Antibiotics 13(10): 942. https://doi.org/10.3390/antibiotics13100942

Bhanderi G.R. 2012. Biology and management of rice weevil, *Sitophilus oryzae* (Linnaeus) on stored sorghum. M.Sc. thesis. Navsari Agricultural University, Navsari, India. 168 p. https://krishikosh.egranth.ac.in/server/api/core/bitstreams/add6f917-0c35-4ac4-a4d7-0791acdec4fc/content

Chaudhari A.K., Singh V.K., Kedia A., Das S., Dubey N.K. 2021. Essential oils and their bioactive compounds as eco-friendly novel green pesticides for management of storage insect pests: Prospects and retrospects. Environmental Science and Pollution Research 28: 18918-18940. https://doi.org/10.1007/s11356-021-12841-w

Chen Q., Hu X., Li J., Liu P., Yang Y., Ni Y. 2011. Preparative isolation and purification of cuminaldehyde and p-mentha-1,4-dien-7-al from the essential oil of *Cuminum cyminum* L. by high-speed counter-current chromatography. Analytica Chimica Acta 689(1): 149-154. https://doi.org/10.1016/j.aca.2011.01.038

Daliri Shamsabadi O. 2023. An overview of the application of nanomaterials and biodegradable polymers in the food packaging industry. Basparesh 13(1): 19-28. (In Farsi). https://doi.org/10.22063/basparesh.2022.3008.1587

Danna C., Malaspina P., Cornara L., Smeriglio A., Trombetta D., De Feo V., Vanin S. 2024. Eucalyptus essential oils in pest control: a review of chemical composition and applications against insects and mites. Crop Protection 176: 106319. https://doi.org/10.1016/j.cropro.2023.106319

Dastranj M., Ghaffari M.R., Bandani A., Hossein Salekdeh G. 2017. Identification of candidate Glutathione S-transferase (GST) genes in Sunn pest, *Eurygaster integriceps* Put. (Hem.: Scutelleridae), using RNA-seq analysis. Journal of Entomological Society of Iran 37(1): 27-42. (In Farsi). https://jesi.areeo.ac.ir/article_109932.html

Demeter S., Lebbe O., Hecq F., Nicolis S.C., Kemene T.K., Martin H., Fauconnier M., Hance T. 2021. Insecticidal activity of 25 essential oils on the stored product pest, *Sitophilus granarius*. Foods 10(2): 200. https://doi.org/10.3390/foods10020200

Doherty E.M., Sun Q., Wilson B.E. 2023. Stored rice varietal resistance towards *Sitophilus oryzae*. Crop Protection 165: 106162. https://doi.org/10.1016/j.cropro.2022.106162

Ellman G.L., Courtney K.D., Andres V., Featherstone R.M. 1961. A new and rapid colorimetric determination of acetylcholinesterase activity. Biochemical Pharmacology 7(2): 88-95. https://doi.org/10.1016/0006-2952(61)90145-9

Habig W.H., Pabst M.J., Jakoby W.B. 1974. Glutathione S-transferases: The first enzymatic step in mercapturic acid formation. Journal of Biological Chemistry 249(22): 7130-7139. https://doi.org/10.1016/S0021-9258(19)42083-8

He X., Chen X., Yang Y., Xie Y., Liu Y. 2024. Medicinal plants for epileptic seizures: Phytoconstituents, pharmacology and mechanisms revisited. Journal of Ethnopharmacology 320: 117386. https://doi.org/10.1016/j.jep.2023.117386

Hosseinzadeh K., Khosrowshahi Asl A., Alizadeh Khaledabad M., Almasi H. 2021. Investigating the effect of film preparation method (composite or laminated) and biopolymersâ proportion on the physicochemical properties of active chitosan-whey protein isolate film by response surface method (RSM). Journal of Food Science and Technology (Iran) 18(113): 59-75. (In Farsi). https://doi.org/10.52547/fsct.18.113.59

Jabbar M., Baboo I., Majeed H., Farooq Z., Palangi V., Lackner M. 2024. Preparation and characterization of cumin essential oil nanoemulsion (CEONE) as an antibacterial agent and growth promoter in broilers: A study on efficacy, safety, and health impact. Animals 14(19): 2860. https://doi.org/10.3390/ani14192860

Jalaeian M., Mohammadzadeh M., Mohammadzadeh M., Borzou E. 2021. Rice cultivars affect fitness-related characteristics and digestive physiology of the rice weevil, *Sitophilus oryzae* (L.) (*Coleoptera: Curculionidae*). Journal of Stored Products Research 93: 101821. https://doi.org/10.1016/j.jspr.2021.101821

Jasman A.K., Slomy A.K., Khaleel A.I. 2025. Nanoemulsion-enhanced insecticidal activity of *Cymbopogon citratus* and *Mentha longifolia* essential oils against the red flour beetle (*Tribolium castaneum*). Journal of Stored Products Research 114: 102759. https://doi.org/10.1016/j.jspr.2025.102759

Jesser E., Castillo L., Alonso Y., Urrutia R.I., Murray A.P., Domini C., Werdin-González J.O. 2022. Development of active biodegradable films based on chitosan and essential oil to prevent infestation of *Plodia interpunctella* (Lepidoptera: Pyralidae). Food Packaging and Shelf Life 34: 100999. https://doi.org/10.1016/j.fpsl.2022.100999

Ji R., Guo H., Yang X., Wang L., Zhang X., Zhang H. 2026. Chitosan/gelatin-based film activated by Pickering emulsion of citrus essential oil stabilized by esterified starch/whey protein isolate fibrils: Application in preserving freshness of blueberry. Food Chemistry 503: 147848. https://doi.org/10.1016/j.foodchem.2026.147848

Johnson A.J., Venukumar V., Varghose T.S., Viswanathan G.L. 2022. Insecticidal properties of *Clausena austroindica* leaf essential oil and its major constituent, trans-anethole, against *Sitophilus oryzae* and *Tribolium castaneum*. Industrial Crops and Products 182: 114854. https://doi.org/10.1016/j.indcrop.2022.114854

Kannan N., Chandrasekaran N. 2026. Encapsulated essential oil-based nanoemulsion beads: A green innovation for storage pest control against *Tribolium castaneum*. RSC Advances 16: 23715-23729. https://doi.org/10.1039/D6RA02377K

Kavallieratos N.G., Bonacucina G., Nika E.P., Skourti A., Georgakopoulou S.K.C., Filintas C.S., Panariti A.M.E., Maggi F., Petrelli R., Ferrati M., Spinozzi E., Perinelli D.R., Canale A., Benelli G. 2023. The type of grain counts: Effectiveness of three essential oil-based nanoemulsions against *Sitophilus oryzae*. Plants 12(4): 813. https://doi.org/10.3390/plants12040813

Lozano-Navarro J.I., Díaz-Zavala N.P., Velasco-Santos C., Martínez-Hernández A.L., Tijerina-Ramos B.I., García-Hernández M., Rivera-Armenta J.L., Páramo-García U., Reyes-de la Torre A.I. 2017. Antimicrobial, optical and mechanical properties of chitosan-starch films with natural extracts. International Journal of Molecular Sciences 18(5): 997. https://doi.org/10.3390/ijms18050997

Marsin A.M., Ida I.M., Anis S.N., Lamiz N.A., Ching L.W., Dolhaji N.H. 2020. Essential oils as insect repellent agents in food packaging: A review. European Food Research and Technology 246: 1519-1532. https://doi.org/10.1007/s00217-020-03511-1

Meybeck A., Cederberg C., Gustavsson J., van Otterdijk R., Sonesson U. 2011. Global food losses and food waste. Food and Agriculture Organization of the United Nations (FAO), Rome, Italy. https://openknowledge.fao.org/handle/20.500.14283/i2697e

Miller L.C., Tainter M. 1944. Estimation of the ED50 and its error by means of logarithmic-probit graph paper. Proceedings of the Society for Experimental Biology and Medicine 57(2): 261-264. https://doi.org/10.3181/00379727-57-14776

Moradi A., Piri R. 2018. Plant growth promoting rhizobacteria enhance salinity stress tolerance in cumin (*Cuminum cyminum* L.) during germination stage. Journal of Plant Process and Function 6(22): 47-54. https://dor.isc.ac/dor/20.1001.1.23222727.1396.6.22.8.2

Msegued Ayam I., Zinedine A., Lyagoubi A., Rocha J.M., Raoui S.M., Errachidi F. 2025. Chemical composition, antioxidant, and antifungal activity of essential oil extracted from cumin seeds (*Cuminum cyminum* L.) planted in Morocco. Chemistry & Biodiversity 22(9): e02687. https://doi.org/10.1002/cbdv.202402687

Nasr Azadani F., Jalali Sendi J., Ebadollahi A., Azizi R., Setzer W.N. 2025. Toxicity and detoxification enzyme inhibition in the two-spotted spider mite (*Tetranychus urticae* Koch) by *Artemisia annua* L. essential oil and its major monoterpenoids. Insects 16(8): 811. https://doi.org/10.3390/insects16080811

Nouri A., Mofasseri M., Jahani R., Ghodrati M., Emam S.M.M., Ebadi M.T. 2024. Phytochemical composition, hypnotic activity, and antinociceptive properties of cumin essential oil collected from various geographical regions. Food Science & Nutrition 12(11): 9025-9034. https://doi.org/10.1002/fsn3.4432

Oliyaei N., Awlqadr F.H., Irajie C., Yazdanpanah S., Zomorodian K., Iraji A. 2026. Preparation and characterization of emulsion-based fucoidan-whey protein film activated with geranium essential oil for food applications. Food Science & Nutrition 14(5): e71811. https://doi.org/10.1002/fsn3.71811

Omar A.F., Khalil F.M.A., Alomran M.M., Ismail T., El-Tokhy A.I., Abdelaal K., Gharsan F.N., Almozini R.N., Abouelatta A.M. 2024. Toxicity and enzymatic activity changes in rice weevil (*Sitophilus oryzae*) induced by basil (*Ocimum basilicum*) and cumin (*Cuminum cyminum*) essential oils. Scientific Reports 14: 28684. https://doi.org/10.1038/s41598-024-80329-x

Peng Q., Huang Z., Liang G., Bi Y., Kong F., Wang Z., Tan S., Zhang J. 2024. Preparation of protein-stabilized *Litsea cubeba* essential oil nano-emulsion by ultrasonication: Bioactivity, stability, in vitro digestion, and safety evaluation. Ultrasonics Sonochemistry 107: 106892. https://doi.org/10.1016/j.ultsonch.2024.106892

Piri A., Sahebzadeh N., Zibaee A., Khani A. 2021. Effect of some botanicals and imidacloprid on the biochemical parameters of red palm weevil (*Rhynchophorus ferrugineus* Olivier). Journal of Iranian Plant Protection Research 35(1): 39-55. (In Farsi). https://doi.org/10.22067/jpp.2021.32849.0

Prabhakar P.R., Reddy J.P., Murthy P.K., Babu C.V. 2024. Insecticidal property of *Ocimum* essential oil embedded polylactic acid packaging films for control of *Sitophilus oryzae* and *Callosobruchus chinensis*. International Journal of Biological Macromolecules 256: 128298. https://doi.org/10.1016/j.ijbiomac.2023.128298

Sandberg H., Alnoor A., Tiberius V. 2023. Environmental, social, and governance ratings and financial performance: Evidence from the European food industry. Business Strategy and the Environment 32(4): 2471-2489. https://doi.org/10.1002/bse.3259

Sheikhi M., Moghimi R., Rezazadeh F. 2025. Development of bio-based nanoemulsion and pickering emulsion systems of eucalyptus essential oil stabilized by Persian Gum-HPMC-chitosan biopolymers: Toward industrial applications in functional films and sustainable biomaterials. Industrial Crops and Products 234: 121642. https://doi.org/10.1016/j.indcrop.2025.121642

Strong R.G., Sbur D.E., Partida G.J. 1967. Rearing stored-product insects for laboratory studies: Lesser grain borer, granary weevil, rice weevil, Sitophilus zeamais, and Angoumois grain moth. Journal of Economic Entomology 60(4): 1078-1082. https://doi.org/10.1093/jee/60.4.1078

Tan W., Dong F., Zhang J., Zhao X., Li Q., Guo Z. 2019. Physical and antioxidant properties of edible chitosan ascorbate films. Journal of Agricultural and Food Chemistry 67(9): 2530-2539. https://doi.org/10.1021/acs.jafc.8b04567

Wang A., Zhang J., Wu L. 2026. Ternary interactions of starch, protein, and polyphenols in constructing composite thermoplastic starch-based edible packaging: Optimization of preparation techniques and investigation of film-formation mechanisms. Foods 15(1): 36. https://doi.org/10.3390/foods15010036

Wang X., Yong H., Gao L., Li L., Jin M., Liu J. 2019. Preparation and characterization of antioxidant and pH-sensitive films based on chitosan and black soybean seed coat extract. Food Hydrocolloids 89: 56-66. https://doi.org/10.1016/j.foodhyd.2018.10.019

Yarahmadi A., Dousti B., Karami-Khorramabadi M., Afkhami H. 2024. Materials based on biodegradable polymers chitosan/gelatin: A review of potential applications. Frontiers in Bioengineering and Biotechnology 12: 1397668. https://doi.org/10.3389/fbioe.2024.1397668

Zhou C.Q., Lu C.H., Mai L., Bao L., Liu L.Y., Zeng E.Y. 2021. Response of rice (*Oryza sativa* L.) roots to nanoplastic treatment at seedling stage. Journal of Hazardous Materials 401: 123412. https://doi.org/10.1016/j.jhazmat.2020.123412

**HOW TO CITE THIS ARTICLE**

Shahnazari M., Jalalizand A., Mahmoudi E. 202x. Development of WPI/Gelatin Active Films Loaded with *Cuminum cyminum* Essential Oil Nanoemulsion for the Control of *Sitophilus oryzae*. *Agrotechniques in Industrial Crops* x(x): xx-xx. 10.22126/ATIC.2027.14251.1296